

Elastic production of Vector Mesons at HERA: study of the scale of the interaction and measurement of the helicity amplitudes ¹

Barbara CLERBAUX
 Université Libre de Bruxelles
 e-mail: barbara.clerbaux@hep.ihe.ac.be

Abstract

A compilation of H1 and ZEUS cross section measurements for elastic vector meson production is presented as a function of the scale $K^2 = (Q^2 + M_V^2)/4$, where Q^2 is the exchanged photon virtuality and M_V is the mass of the vector meson. The ratio of longitudinal to transverse cross sections $R = \sigma_L/\sigma_T$ is presented as a function of Q^2/M_V^2 . The cross sections are separated in a transverse and a longitudinal component and are presented as a function of the scale K^2 . The intercept $\alpha(0) - 1$ governing the energy dependence of the vector meson cross sections is compared with the λ parameter measured in inclusive F_2 analysis. For ρ meson production, the helicity amplitude ratios $|T_{ij}|/|T_{00}|$, extracted from the H1 and ZEUS measurements of the spin density matrix elements are presented as a function of Q^2 and W and are compared to recent predictions.

1 Introduction

This note includes the most recent HERA results on exclusive vector meson (VM) production: $e + p \rightarrow e + VM + p$. The H1 and ZEUS experiments studied the production of ρ [1–4], ω [5,6], ϕ [7–9], J/ψ [3,10–12] and Υ [13,14] mesons, in a Q^2 domain ranging from photoproduction ($Q^2 \simeq 0$) to $Q^2 = 60 \text{ GeV}^2$ (where Q^2 is the virtuality of the photon exchanged in the interaction).

The note is divided in two parts. The first part presents the Q^2 and W dependences of the total, transverse and longitudinal cross sections, for the various vector mesons. The second part is concerned only with ρ meson production, and presents measurements of the helicity amplitude ratios $|T_{ij}|/|T_{00}|$.

¹ Plots presented in the vector meson discussion session of the Workshop of Low- x Physics (June 1999) in Tel-Aviv, Israel.

2 The cross section $\sigma(\gamma^{(*)}p \rightarrow VM p)$

2.1 Scale of the interaction

Recent measurements of ρ meson electroproduction at $Q^2 \gtrsim 10 \text{ GeV}^2$ [1, 3] and of J/ψ meson photo- and electroproduction [3, 10, 11] indicate a strong energy dependence of the $\gamma^{(*)}p \rightarrow VM p$ cross sections (“hard” behaviour): $\sigma \propto W^\delta$ with $\delta \simeq 0.8$, where W is the energy in the photon-proton centre of mass. This behaviour indicates that the mass of the c quark or a high Q^2 value provides a “scale” K^2 in the interaction. In this section, results are presented for all VM production in a global way as a function of the scale $K^2 = (Q^2 + M_V^2)/4$, where M_V is the VM mass. This approach is inspired e.g. by the discussions in reference [15].

A compilation of the HERA measurement of the $\gamma^{(*)}p \rightarrow VM p$ cross sections is presented in Fig. 1 as a function of $(Q^2 + M_V^2)/4$. The cross sections were scaled by SU(4) factors, according to the quark content of the VM : *9/1 for the ω , *9/2 for the ϕ , *9/8 for the J/ψ and *9/2 for the Υ mesons. In Fig. 1 and in all following plots, the errors on the data points represent the full errors (including the statistical, systematic and normalisation errors, added in quadrature).

The cross sections are measured at $W = 75 \text{ GeV}$, or are moved to this value according to the parametrisation $\sigma \propto W^\delta$, using the δ value measured by the relevant experiment. The ZEUS ρ and ϕ cross sections were corrected for the $|t|$ cut ($|t| < 0.5$ or 0.6 GeV^2), following an exponentially falling distribution $d\sigma/dt \propto e^{bt}$, with a Q^2 dependent b parameter according to measurements (this correction is $\lesssim 7 \%$).

Within experimental errors, the total cross sections for VM production, including the SU(4) normalisation factors, appear to lay on a universal curve when plotted as a function of the scale $K^2 = (Q^2 + M_V^2)/4$, except possibly for the Υ photoproduction ².

A fit performed on the H1 and ZEUS ρ data using the parametrisation $\sigma = a(K^2 + b^2)^c$, with $b^2 = 0.11 \pm 0.03 \text{ GeV}^2$ and $c = -2.37 \pm 0.10$ ($\chi^2/ndf = 0.67$) is shown as the full curve in Fig. 1. The ratio of the ω , ϕ and J/ψ cross sections to this parametrisation is presented in the lower plot of Fig. 1.

It is interesting to recognise that the universal $(Q^2 + M_V^2)/4$ dependence is for the total cross section measurements.

2.2 Ratio of the longitudinal to transverse cross sections

The measured ratio of longitudinal to transverse cross sections $R = \sigma_L/\sigma_T$ at $Q^2 = 6 \text{ GeV}^2$ is approximately 2.5 for ρ meson production but approximately 0.4 for J/ψ meson production.

²The cross sections $\sigma(\gamma p \rightarrow \Upsilon(1S)p)$ measured by H1 and ZEUS at $W = 160$ and 120 GeV respectively, were moved to the value $W = 75 \text{ GeV}$ using the parametrisation $\sigma \propto W^\delta$, with $\delta = 1.7$. This high value of the parameter δ comes from the prediction of [16]. Note that if the value $\delta = 0.8$ is used (a value measured in case of J/ψ photoproduction), the cross sections are higher by a factor 1.5 for ZEUS and 2.0 for H1.

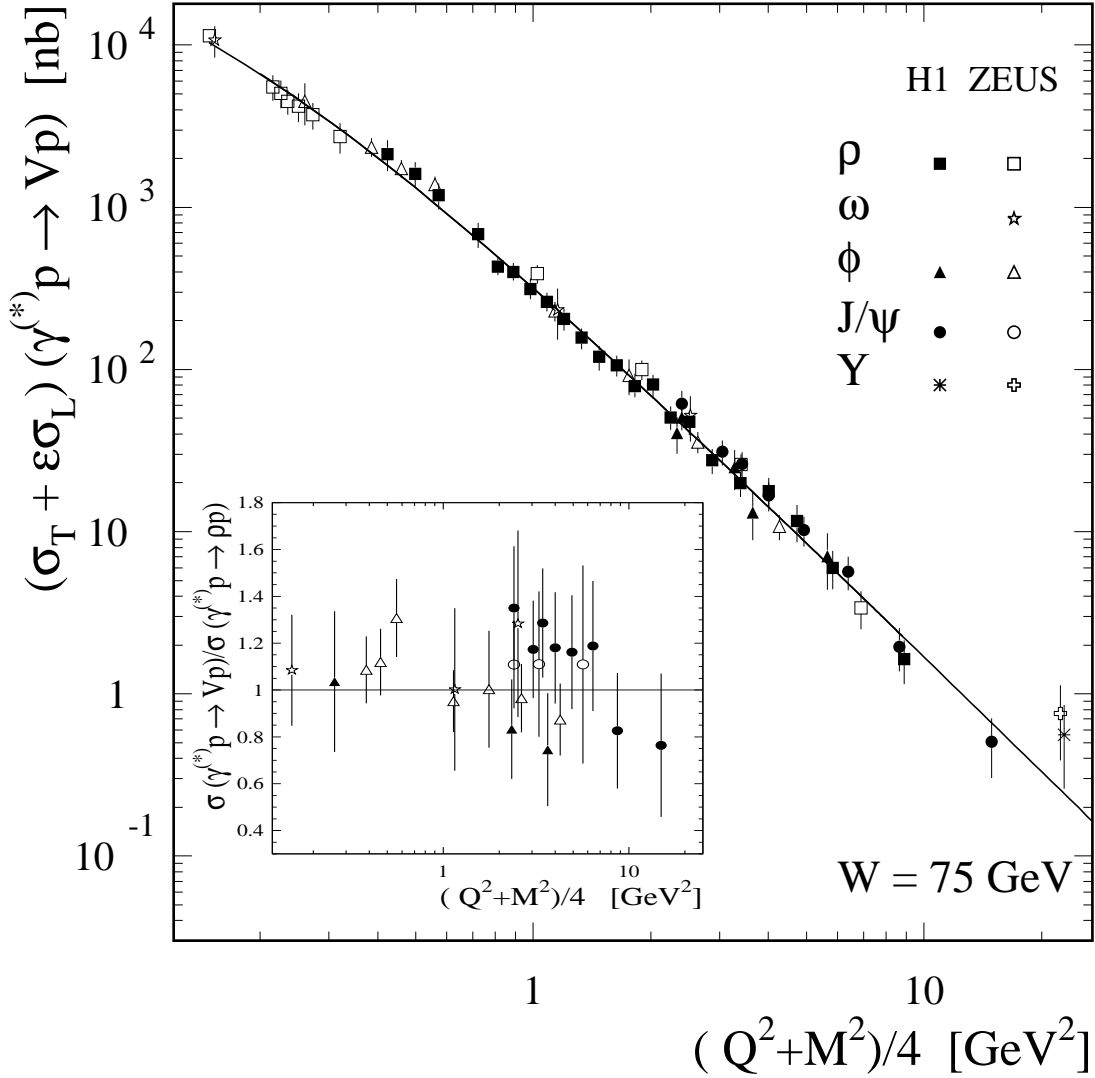


Figure 1: H1 and ZEUS measurements of the total cross sections $\sigma(\gamma p^{(*)} \rightarrow VM p)$ as a function of $(Q^2 + M_V^2)/4$ for ρ , ω , ϕ , J/ψ and Υ vector meson elastic production, at the fixed value of $W = 75$ GeV [1–14]. The error bars represent the total errors. The curve corresponds to a fit to the H1 and ZEUS ρ data.

However, the ratio R presents a similar dependence for the ρ , ϕ and J/ψ meson production when plotted as a function of Q^2/M_V^2 (see Fig. 2). All data are well described by a common empirical parametrisation: $R = a(Q^2/M_V^2)^b(\ln Q^2/M_V^2 + 10)^c$ (curve in Fig. 2).

It is observed that R rises steeply at small Q^2 , with a weaker dependence at large Q^2 values. This behaviour is consistent with the fact that the Q^2/M_V^2 dependence expected at leading order is modified by higher order corrections. The data in Fig. 2 suggest that, within the present statistical precision, this modification preserves the ratio Q^2/M_V^2 as the relevant variable for σ_L/σ_T .

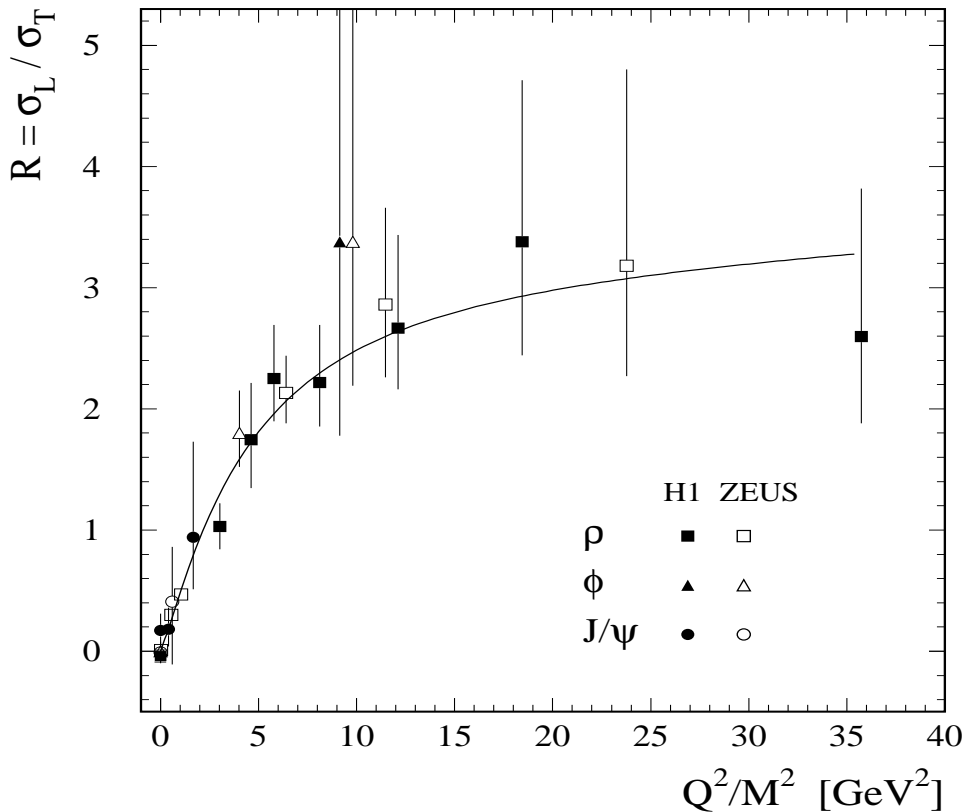


Figure 2: H1 and ZEUS measurements of $R = \sigma_L/\sigma_T$ as a function of Q^2/M_V^2 , for ρ , ϕ and J/ψ vector meson elastic production [1–3,8–12]. The error bars represent the total errors. The curve corresponds to the fit presented in the text.

2.3 The transverse and longitudinal cross sections

Figs. 3 (a) and (b) present the transverse σ_T and the longitudinal σ_L cross sections separately, as a function of $(Q^2 + M_V^2)/4$. The parametrisation for $R = \sigma_L/\sigma_T$, described above, was used to separate the longitudinal and the transverse parts of the cross sections for the different vector mesons:

$$\sigma = \sigma_T + \varepsilon\sigma_L = \sigma_T(1 + \varepsilon R),$$

where the polarisation parameter $\langle\varepsilon\rangle = 0.996$ at HERA.

The transverse cross sections are well described by a simple power law dependence: $\sigma_T \propto (Q^2 + M_V^2)^n$, with $n = -2.47 \pm 0.03$ for ρ , $n = -2.4 \pm 0.1$ for ω , $n = -2.8 \pm 0.1$ for ϕ , and $n = -3.1 \pm 0.2$ for J/ψ meson production.

In view of these values of the parameter n ($n \neq 2$), the parametrisation proposed in the GVDM approach of Schildknecht, Schuler and Surrow [17] does not provide good fits³.

2.4 Energy dependence

The energy dependence of the cross section for VM production at HERA can be parametrised as $\sigma \propto W^\delta$. In a Regge context, the parameter δ can be related to the exchanged trajectory $\alpha(t)$, which is assumed to take a linear form $\alpha(t) = \alpha(0) + \alpha' t$, where t is the square of the four-momentum exchanged at the proton vertex. The value $\alpha' = 0.25 \text{ GeV}^{-2}$ is assumed for the ρ and ϕ mesons, as measured in hadron-hadron interactions [20]. For the J/ψ meson, the value $\alpha' = 0.05$ is used [10].

The values obtained for the parameter $(\alpha(0) - 1)$ for the ρ , ϕ and J/ψ meson production are presented in Fig. 4 as a function of the scale $K^2 = (Q^2 + M_V^2)/4$. The error bars on the data represent the full errors. For the ρ meson production, the sensitivity to the choice of α' is shown by the outer bars, which contain the variation due to the assumption $\alpha' = 0$ (i.e. no shrinkage) added in quadrature. The points are compared to the values of the parameter λ obtained from fits to the W dependence of inclusive F_2 measurements [18] ($\sigma_{tot} \propto F_2(x, Q^2) \propto (1/x)^\lambda \propto W^{2\lambda}$), plotted as a function of the scale $K^2 = Q^2$ (see also [19]).

Within experimental errors, a common rise is observed for the $(\alpha(0) - 1)$ and the λ parameters when plotted as a function of the relevant scale K^2 . This is at variance with the values 1.08–1.10 obtained from fits to the total and elastic hadron-hadron cross sections [20, 21].

³If the transverse and the longitudinal cross sections are fitted using the Schildknecht, Schuler and Surrow parametrisation, one obtains for the square of the transverse masses $0.29 \pm 0.01 \text{ GeV}^2$ ($\chi^2/ndf = 3.6$), $0.39 \pm 0.03 \text{ GeV}^2$ ($\chi^2/ndf = 5.7$) and $4.1 \pm 0.4 \text{ GeV}^2$ ($\chi^2/ndf = 1.9$) for the ρ , ϕ and J/ψ mesons respectively. The results for the square of the longitudinal masses are $0.38 \pm 0.02 \text{ GeV}^2$ ($\chi^2/ndf = 3.1$), $0.53 \pm 0.05 \text{ GeV}^2$ ($\chi^2/ndf = 2.2$) and $5.4 \pm 0.7 \text{ GeV}^2$ ($\chi^2/ndf = 0.8$) for the ρ , ϕ and J/ψ mesons respectively.

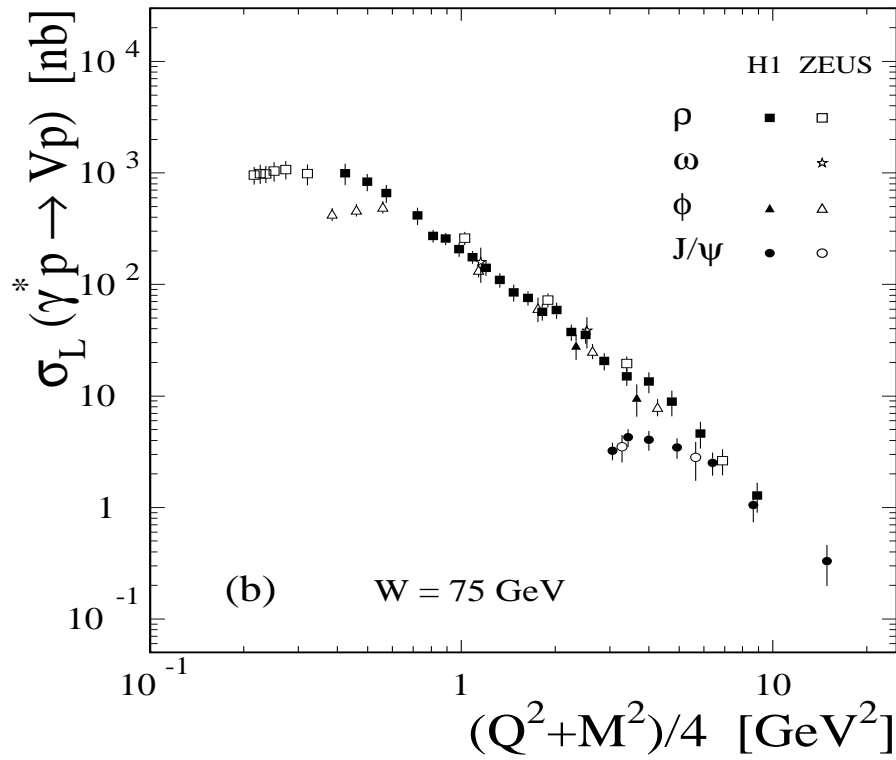
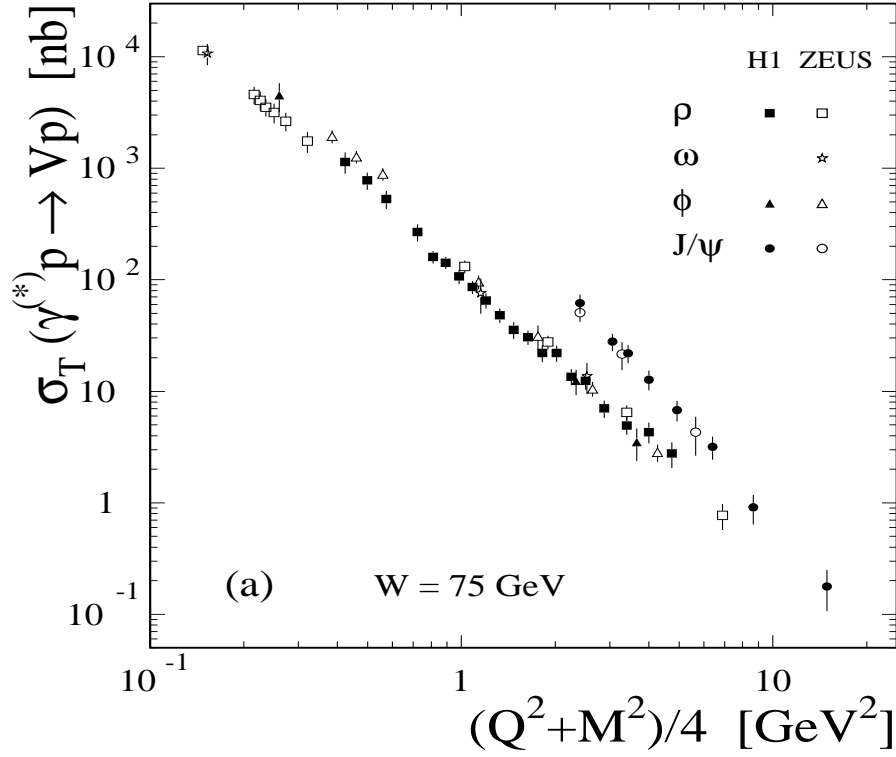


Figure 3: H1 and ZEUS measurements of the longitudinal (a) and the transverse (b) cross sections as a function of $(Q^2 + M_V^2)/4$ for ρ , ω , ϕ and J/ψ vector meson elastic production, at the fixed value of $W = 75 \text{ GeV}$ [1–12]. The error bars represent the total errors.

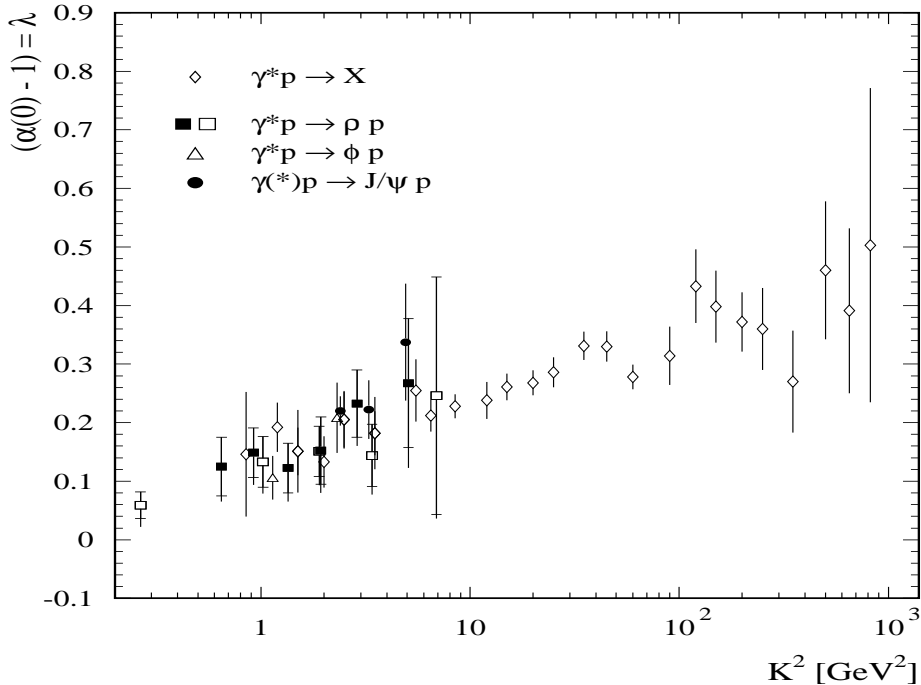


Figure 4: The parameter $(\alpha(0) - 1)$ and λ as a function of the scale K^2 . The H1 [1,10,11] and ZEUS [3,9] measurements for elastic vector meson production are labelled as in Fig. 1. The inclusive F_2 measurements from H1 [18] are labelled using open diamonds. The error bars on the data represent the full errors. For ρ meson production, the outer bars correspond to the case $\alpha' = 0$. The scale is $K^2 = Q^2$ for the F_2 inclusive measurement and $K^2 = (Q^2 + M_V^2)/4$ for elastic vector meson production.

3 Helicity amplitudes

This section presents the H1 and ZEUS elastic ρ meson production results on the study of angular distributions of the ρ meson production and decay [1,4], which provides information on the photon and ρ polarisation.

Following the formalism of [22], the normalised angular decay distribution is a function of 15 combinations of spin density matrix elements, $r_{ij}^{\alpha\beta}$. Each of these $r_{ij}^{\alpha\beta}$ is a sum of bilinear combinations of the helicity amplitudes $T_{\lambda\rho\lambda\gamma}$. One can thus invert the system and extract the helicity amplitudes from the measurement of the 15 elements. The motivations for extracting the helicity amplitudes from the 15 matrix elements are the following:

1. fundamental quantities are computed, on which s -channel helicity conservation ⁴ (SCHC)

⁴ In case of s -channel helicity conservation (SCHC), the helicity of the vector meson is equal to that of the

hypothesis can be checked directly,

2. measurements of the real and imaginary parts of the helicity amplitudes can be obtained.

Only 15 equations are available for 18 unknowns (9 complex helicity amplitudes $T_{\lambda_\rho\lambda_\gamma} = |T_{\lambda_\rho\lambda_\gamma}|e^{i\varphi_{\lambda_\rho\lambda_\gamma}}$). However, both H1 [1] and ZEUS [4] results are compatible with natural parity exchange⁵ (NPE). Under this hypothesis, 5 helicity amplitudes remain independent (10 unknown): $T_{00}, T_{11}, T_{01}, T_{10}$ and T_{1-1} .

3.1 The ratios $|T_{ij}|/|T_{00}|$

Minimum χ^2 fits were performed to measurements of the combinations of the matrix element to extract the 5 independent complex helicity amplitudes. The normalisation $|T_{00}| = 1$ and $\varphi_{00} = 0$ is used. In the full fit, the parameters $|T_{1-1}|$, φ_{10} , φ_{01} and φ_{1-1} were found compatible with zero within large errors. These parameters are then put to zero, and the remaining free parameters of the fit are $|T_{11}|$, $|T_{01}|$, $|T_{10}|$ and φ_{11} .

The measurement of the ratios $|T_{11}|/|T_{00}|$, $|T_{01}|/|T_{00}|$ and $|T_{10}|/|T_{00}|$ as a function of Q^2 is presented in Figs. 5 (a), (b) and (c) respectively (see also table 1). The H1 data cover the kinematic range $2.5 < Q^2 < 60 \text{ GeV}^2$, $30 < W < 140 \text{ GeV}$ ($\langle W \rangle = 75 \text{ GeV}$) and $\langle |t| \rangle = 0.138 \text{ GeV}^2$. For the ZEUS data, the kinematic domain is $0.25 < Q^2 < 0.85 \text{ GeV}^2$, $20 < W < 90 \text{ GeV}$ ($\langle W \rangle = 45 \text{ GeV}$) and $\langle |t| \rangle = 0.14 \text{ GeV}^2$ for the low Q^2 data and $3 < Q^2 < 30 \text{ GeV}^2$, $40 < W < 120 \text{ GeV}$ ($\langle W \rangle = 73 \text{ GeV}$) and $\langle |t| \rangle = 0.17 \text{ GeV}^2$ for the high Q^2 data.

The ratio $|T_{11}|/|T_{00}|$ decreases when Q^2 increases, indicating that at high Q^2 longitudinal polarisation dominates. The ratio $|T_{01}|/|T_{00}|$ is observed to be around 8 % (14.0 σ from zero, 5 data points), and the ratio $|T_{10}|/|T_{00}|$ around 3 – 4 % (4.5 σ from zero), which indicate a small but significant violation of SCHC for ρ meson production at HERA.

The predictions of three models based on perturbative QCD are compared to the HERA measurements in Fig. 5. The dashed lines represent the predictions of the Royen and Cudell model [23], computed for $\langle |t| \rangle = 0.135 \text{ GeV}^2$. The dotted lines are the predictions of the Nikolaev and Akushevich model [24], for $\langle |t| \rangle = 0.13 \text{ GeV}^2$ and $\langle W \rangle = 75 \text{ GeV}$. The dash-dotted and full lines present the predictions of the Ivanov and Kirschner model [25], computed for $\langle |t| \rangle = 0.13 \text{ GeV}^2$ and $\langle W \rangle = 75 \text{ GeV}$, using respectively the GRV94HO and the CTEQ41Q parametrisations for the gluon density in the proton. These three models predict a violation of SCHC, the amplitudes T_{01} and T_{10} being different from zero, in agreement with the data.

The W dependence of the ratios $|T_{ij}|/|T_{00}|$ is presented in Figs. 6 (a), (b) and (c) for $\langle Q^2 \rangle = 4.8 \text{ GeV}^2$, together with predictions of the Nikolaev and Akushevich model [24] (dotted lines) and the Ivanov and Kirschner model [25] (dash-dotted and full lines) (the Royen and Cudell model gives no prediction for the W dependence).

photon when the spin quantisation axis is taken along the direction of the meson momentum is the γ^*p centre of mass system. In that case, the non-flip helicity amplitudes $T_{\lambda_\rho\lambda_\gamma} = T_{00}$ and T_{11} have non-zero values, the single flip ($T_{10}, T_{01}, T_{0-1}, T_{-10}$) and double flip amplitudes (T_{1-1}, T_{-11}) being zero.

⁵ Natural parity exchange (NPE) is defined by the following relations between the helicity amplitudes: $T_{-\lambda_\rho-\lambda_\gamma} = (-1)^{\lambda_\rho-\lambda_\gamma} T_{\lambda_\rho\lambda_\gamma}$.

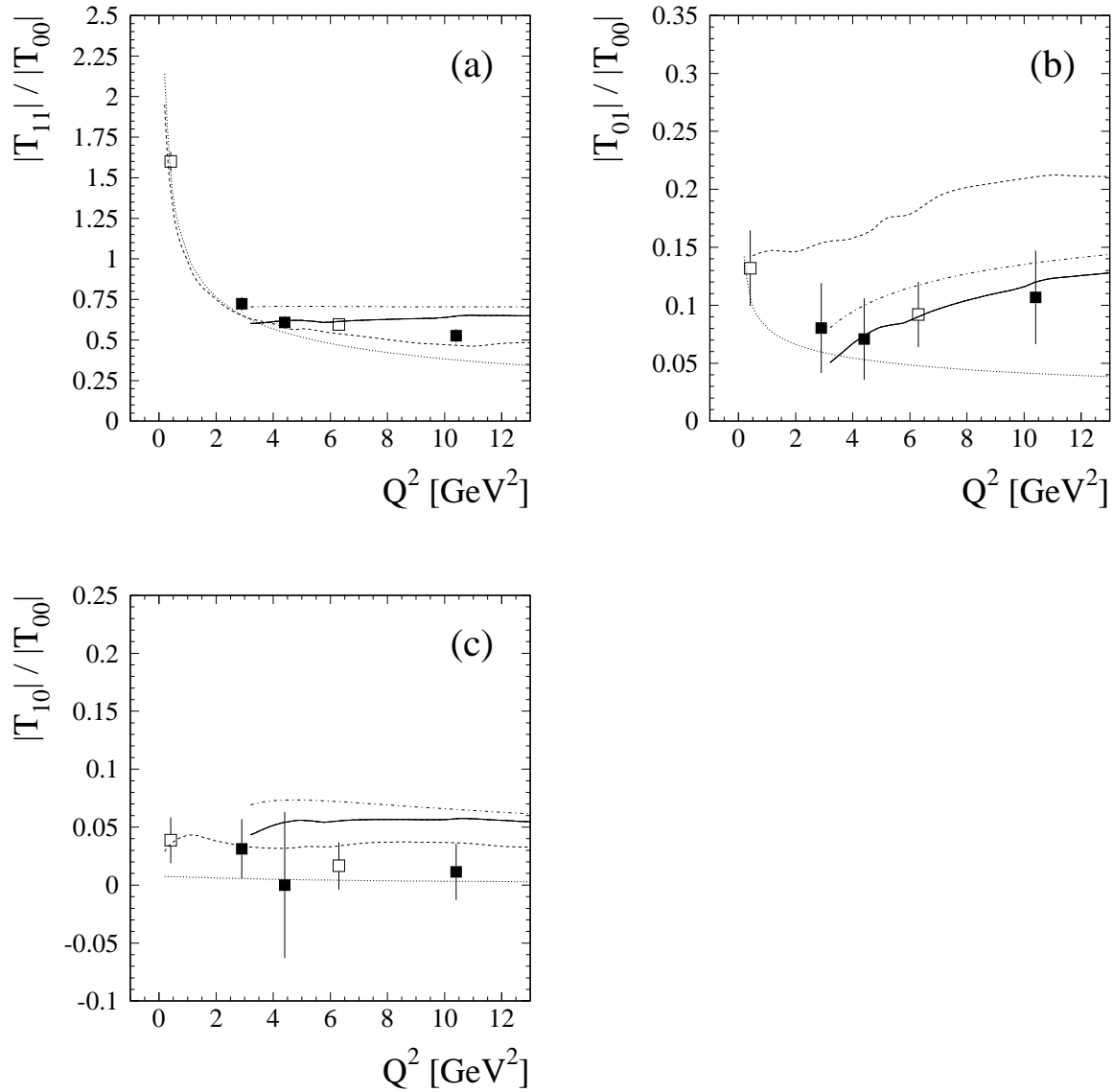


Figure 5: Q^2 dependence of the ratio of the helicity amplitudes: $|T_{11}|/|T_{00}|$ (a), $|T_{01}|/|T_{00}|$ (b) and $|T_{10}|/|T_{00}|$ (c), extracted from the H1 and ZEUS measurements of the 15 combinations of spin density matrix elements [1, 4]. The dashed and the dotted lines correspond to predictions of the Royen and Cudell model [23] and of the Nikolaev and Akushevich model [24] respectively. The dash-dotted and full lines represent the predictions of the Ivanov and Kirschner model [25] using respectively the GRV94HO and the CTEQ4lQ parametrisations for the gluon density in the proton.

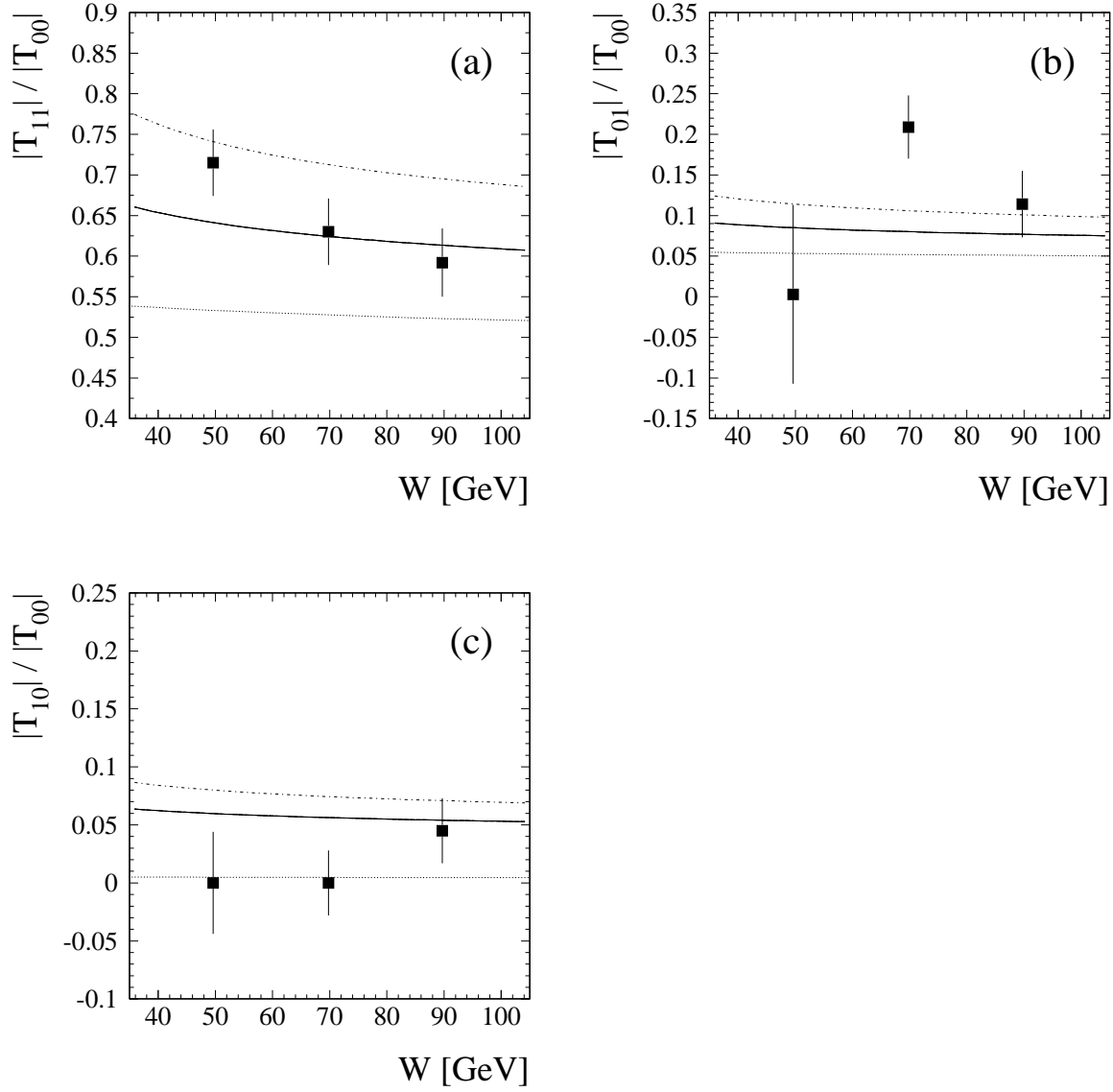


Figure 6: W dependence of the ratio of the helicity amplitudes: $|T_{11}|/|T_{00}|$ (a), $|T_{01}|/|T_{00}|$ (b) and $|T_{10}|/|T_{00}|$ (c), extracted from the H1 measurements of the 15 combinations of spin density matrix elements [1]. The dotted lines correspond to predictions of the Nikolaev and Akushevich model [24]. The dash-dotted and full lines represent the predictions of the Ivanov and Kirschner model [25] using respectively the GRV94HO and the CTEQ41Q parametrisations for the gluon density in the proton.

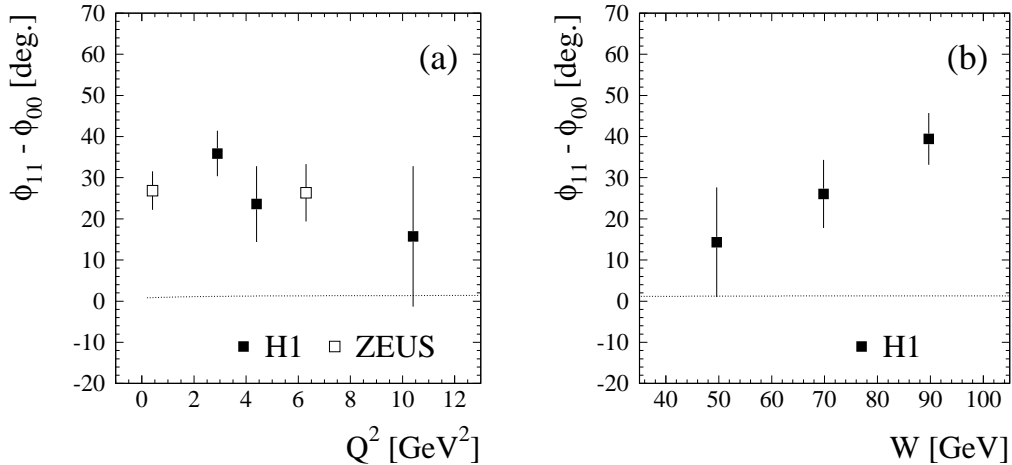


Figure 7: (a) Q^2 and (b) W dependences of the phase difference $\varphi_{11} - \varphi_{00}$ extracted from the H1 and ZEUS measurements of the 15 combinations of spin density matrix elements [1, 4]. The dotted lines correspond to predictions of the Nikolaev and Akushevich model [24].

3.2 The phase $\varphi_{11} - \varphi_{00}$

Figs. 7 (a) and (b) present results for the phase difference $\varphi_{11} - \varphi_{00}$, as a function of Q^2 and W respectively (see also table 1). The phase difference is clearly different from zero, of the order of $\phi = 25$ degrees. This value is in agreement with the H1 measurement [1] of $\cos \phi = 0.925 \pm 0.022$ $^{+0.011}_{-0.022}$ obtained from the angular distribution when supposing SCHC and NPE. The dotted lines on Figs. 7 (a) and (b) represent the predictions of the Nikolaev and Akushevich model [24] ⁶.

3.3 Fixed target experiments

The same procedure was used to extract the helicity amplitudes for the fixed target experiments for which the full set of matrix elements have been measured. The data in references [26], [27] and [28] correspond to Q^2 values between 0.4 and 1.1 GeV^2 and W values between 2.0 and 3.1 GeV, the CHIO experiment [29] is at higher energy ($0 < Q^2 < 3 \text{ GeV}^2$ and $12.5 < W < 16 \text{ GeV}$). The fitted helicity amplitudes for [26] are affected by large errors. Fits to the data in reference [27] have a very bad χ^2 . Fits to the data in reference [28] and to the CHIO data [29] give helicity amplitude ratios in agreement, within the experimental errors, with the Royen and Cudell predictions. The experimental errors on the helicity ratios for these two fixed target experiments are typically a factor five greater than the errors on the HERA measurements.

⁶ The models of Royen and Cudell and of Ivanov and Kirschner suppose that the amplitudes are purely imaginary.

Acknowledgements

I am grateful to I. Akushevich, D. Ivanov, P. Marage, N. Nikolaev, I. Royen for numerous interesting discussions.

Q^2 (GeV ²)	$ T_{11} / T_{00} $	$ T_{01} / T_{00} $	$ T_{10} / T_{00} $	$\varphi_{11} - \varphi_{00}$ (deg.)
0.41	1.601 ± 0.058	0.132 ± 0.033	0.039 ± 0.020	26.9 ± 4.7
2.9	0.723 ± 0.041	0.080 ± 0.039	0.031 ± 0.025	35.9 ± 5.5
4.4	0.608 ± 0.039	0.071 ± 0.035	0.000 ± 0.063	23.6 ± 9.2
6.3	0.595 ± 0.029	0.092 ± 0.028	0.017 ± 0.020	26.3 ± 7.0
10.4	0.526 ± 0.042	0.107 ± 0.040	0.011 ± 0.024	15.7 ± 17.1

Table 1: Ratios of helicity amplitudes $|T_{11}|/|T_{00}|$, $|T_{01}|/|T_{00}|$, $|T_{10}|/|T_{00}|$ and phase difference $\varphi_{11} - \varphi_{00}$, for five Q^2 values, extracted from the H1 and ZEUS measurements of the 15 combinations of spin density matrix elements [1, 4].

References

- [1] H1 Coll., *Elastic Electroproduction of ρ Mesons at HERA*, DESY-99-010, subm. to *Eur. Phys. J. C*, hep-ph/9902019.
- [2] J. Breitweg et al., ZEUS Coll., *Eur. Phys. J.* **C2** (1998) 247.
- [3] J. Breitweg et al., ZEUS Coll., *Eur. Phys. J.* **C6** (1999) 603.
- [4] ZEUS Coll., *Measurement of the Spin-Density Matrix Elements in Exclusive Electroproduction of ρ Mesons at HERA*, DESY-99-102, subm. to *Eur. Phys. J. C*, hep-ph/9908026.
- [5] M. Derrick et al., ZEUS Coll., *Zeit. Phys.* **C73** (1996) 73.
- [6] ZEUS Coll., *Study of the Diffractive Production of Vector Mesons at Large Q^2 or at Large $|t|$ at HERA*, subm. to the Int. Europhys. Conf. on HEP, Tampere, Finland, 1999.
- [7] C. Adloff et al., H1 Coll., *Zeit. Phys.* **C75** (1997) 607.
- [8] M. Derrick et al., ZEUS Coll., *Phys. Lett.* **B377** (1996) 259.
- [9] ZEUS Coll., *Exclusive Electroproduction of ϕ Mesons at HERA*, subm. to the Int. Conf. on HEP, Vancouver, Canada, 1998.
- [10] H1 Coll., *Diffractive J/ψ Photoproduction*, subm. to the Int. Europhys. Conf. on HEP, Tampere, Finland, 1999.

- [11] H1 Coll., *Charmonium Production in Deep Inelastic Scattering at HERA*, DESY-99-026, subm. to *Eur. Phys. J. C*, hep-ph/9903008.
- [12] J. Breitweg et al., ZEUS Coll., *Zeit. Phys.* **C75** (1997) 215.
- [13] H1 Coll., *Photoproduction of Υ Mesons at HERA*, subm. to the Int. Conf. on HEP, Vancouver, Canada, 1998.
- [14] J. Breitweg et al., ZEUS Coll., *Phys. Lett.* **B437** (1998) 432.
- [15] J. Nemchik, N.N. Nikolaev and B.G. Zakharov, *Phys. Lett.* **B341** (1994) 228.
- [16] L.L. Frankfurt, M.F. McDermott and M. Strikman, hep-ph/9812316.
- [17] D. Schildknecht, G.A. Schuler and B. Surrow, *Phys. Lett.* **B449** (1999) 328.
- [18] S. Aid et al., H1 Coll., *Nucl. Phys.* **B470** (1996) 3;
C. Adloff et al., H1 Coll., *Nucl. Phys.* **B497** (1997) 3.
- [19] M. Genovese, proc. of DIS and QCD 6th Int. Workshop, Brussels, April 1998, eds. Gh. Coremans and R. Roosen, p.294.
- [20] A. Donnachie and P.V. Landshoff, *Phys. Lett.* **B296** (1992) 227.
- [21] J.-R. Cudell, K. Kang and S. Kim, *Phys. Lett.* **B395** (1997) 311.
- [22] K. Schilling and G. Wolf, *Nucl. Phys.* **B61** (1973) 381.
- [23] I. Royen and J.-R. Cudell, *Nucl. Phys.* **B545** (1999) 505;
I. Royen, private communication.
- [24] I.P. Ivanov and N.N. Nikolaev, *JETP Lett.* **69** (1999) 294;
E.V. Kuraev, N.N. Nikolaev and B.G. Zakharov, *JETP Lett.* **68** (1998) 696;
I.V. Akushevich, I.P. Ivanov, N.N. Nikolaev and A.V. Pronyaev, private communication.
- [25] D.Yu. Ivanov and R. Kirschner, *Phys. Rev.* **D59** (1998) 114026.
- [26] V. Eckardt et al., *Nucl. Phys.* **B55** (1973) 45.
- [27] P. Joos et al., *Nucl. Phys.* **B113** (1976) 53.
- [28] C. del Papa et al., *Phys. Rev.* **D19** (1979) 1303.
- [29] W.D. Shambroom et al., CHIO Coll., *Phys. Rev.* **D26** (1982) 1.